

# Chemical Shift Tensors of Directly Bonded Phosphorus Nuclei in Unsaturated Four-Membered Rings. Solid-State $^{31}\text{P}$ NMR and Theoretical Study of Trans- and Cis-Substituted Diphosphetes

Guy M. Bernard,<sup>†</sup> Gang Wu,<sup>†,‡</sup> Michael D. Lumsden,<sup>†</sup> Roderick E. Wasylshen,<sup>\*,†</sup> Nicole Maigrot,<sup>§</sup> Claude Charrier,<sup>§</sup> and François Mathey<sup>§</sup>

Department of Chemistry, Dalhousie University, Halifax, Nova Scotia, Canada B3H 4J3, and DCPH-Ecole Polytechnique, 91128 Palaiseau Cedex, France

Received: October 21, 1998; In Final Form: December 18, 1998

The chemical shift (CS) tensors of two four-membered heterocyclic diphosphetes, *trans*- and *cis*-1,2-dihydro-1-methyl-2-phenyl-3,4-bis(*tert*-butyl)-1,2-diphosphete, have been investigated by solid-state  $^{31}\text{P}$  NMR spectroscopy. The dipolar chemical shift method has been employed to determine the magnitudes of the principal components of the  $^{31}\text{P}$  CS tensors in these compounds, as well as their orientations relative to the  $^{31}\text{P}$ – $^{31}\text{P}$  dipolar vector. The spans of the phenyl- and methyl-substituted phosphorus CS tensors of the *trans* isomer are 248 and 280 ppm, respectively, significantly larger than the corresponding values for the *cis* isomer, 139 and 173 ppm. The orientations of the CS tensors in the molecular framework are proposed on the basis of *ab initio* calculations using the gauge-independent atomic orbitals method. The combined experimental–theoretical results suggest that, for both the *trans* and *cis* isomers, the least shielded principal components,  $\delta_{11}$ , are oriented in the plane defined by the four-membered ring. For the *trans* isomer, the most shielded principal components,  $\delta_{33}$ , are approximately perpendicular to this plane; however, for the *cis* isomer, it is the  $\delta_{22}$  components that are perpendicular to the plane of the four-membered ring. The spectra of magic-angle spinning samples of the *trans* isomer exhibit asymmetric, spinning-frequency dependent line shapes, while those of the *cis* isomer are invariant to spinning frequency. These observations are consistent with the CS tensors derived from the  $^{31}\text{P}$  NMR spectra of stationary samples.

## Introduction

Isotropic phosphorus chemical shielding has been studied extensively in solutions.<sup>1–3</sup> Nevertheless, the origins of the observed shielding are not well understood.<sup>4,5</sup> In general, second-rank tensors are required to describe chemical shielding interactions. The symmetric portion of these tensors may be described by three principal components and three angles describing the orientation of the principal axis system (PAS). Any serious effort to understand chemical shielding requires the investigation of these tensors as opposed to their isotropic averages. Solid-state NMR is ideally suited for the characterization of the symmetric portion of chemical shielding tensors and can also provide some information on the orientation of the principal components.<sup>6–8</sup>

The sensitivity of nuclear shielding to variations in molecular structure is dramatic, particularly for phosphorus in strained environments such as those found in cyclic systems. The chemical shielding range of most cyclic phosphines in solution is approximately 350 ppm, much greater than the approximately 120 ppm range observed for the corresponding acyclic compounds.<sup>2</sup> Extreme examples of shielding and deshielding have been found in cyclic systems. For example,  $\delta_{\text{iso}} = -488$  ppm for the  $\text{P}_4$  tetrahedron, which consists of strained three-membered rings.<sup>9</sup> In contrast, some of the least shielded values

for tertiary phosphines have been reported for bridging  $^{31}\text{P}$  nuclei in five-membered bicyclic systems.<sup>10</sup> For  $^{31}\text{P}$  NMR in general, the nuclear shielding of phosphorus in cyclic systems is not fully understood, although the effects of a localized electron lone pair on the observed chemical shifts are thought to be important.<sup>11</sup> A recent study suggests that the lone-pair electrons are delocalized significantly in heterocyclic systems.<sup>12</sup> To investigate the effect of the lone-pair electrons on the observed shielding, Chesnut and Quin undertook a theoretical study of cyclic phosphines.<sup>13</sup> One conclusion of this study is that the deshielded phosphorus in the phospholide ion **1**, 126 ppm relative to that of the phosphole,<sup>14</sup> **2** (Chart 1), is due to the fact that the lone-pair electrons of the ion lie in the ring plane. In this orientation, the energy of the molecular orbitals containing the lone-pair electrons is closer to that of the lowest unoccupied molecular orbital. On the basis of traditional nuclear shielding theory,<sup>15–18</sup> a small orbital energy difference between occupied and unoccupied orbitals may lead to deshielding. Hence, the deshielding of phosphorus in the phospholide ion is explained without resorting to arguments about delocalization of lone-pair electrons.<sup>13</sup>

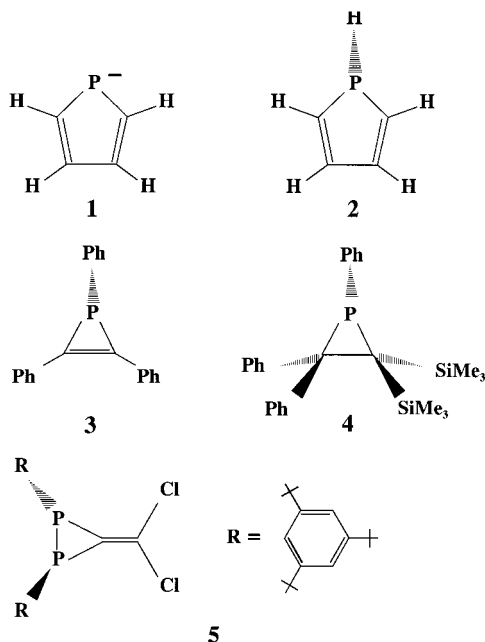
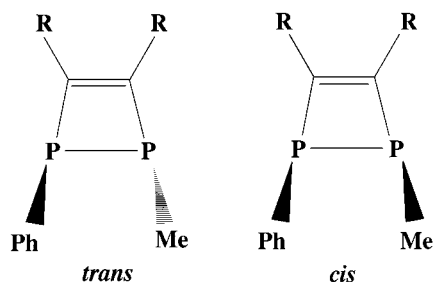
The chemical shielding tensor describes the shielding relative to a bare nucleus. Experimentally, one measures a chemical shift (CS) tensor relative to a given reference, 85%  $\text{H}_3\text{PO}_4$  for phosphorus. Although  $^{31}\text{P}$  CS tensors have been reported for phosphorus nuclei in a variety of environments,<sup>19</sup> only a few of these involve  $^{31}\text{P}$  nuclei in strained-ring systems. Barra and Robert have investigated the  $^{31}\text{P}$  CS tensors of 1,2,3-triphenylphosphirene,<sup>20</sup> **3**, and 1,2,2-triphenyl-3,3-bis(trimethylsilyl)-

\* To whom correspondence should be addressed. Phone: (902) 494-2564. Fax: (902) 494-1310. E-mail: RODW@IS.DAL.CA.

<sup>†</sup> Dalhousie University.

<sup>‡</sup> Present address: Department of Chemistry, Queen's University, Kingston, Ontario, Canada K7L 3N6.

<sup>§</sup> DCPH-Ecole Polytechnique.

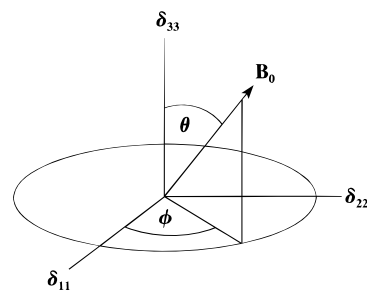
**CHART 1: Molecular Structures of Some Heterocyclic Phosphorus Compounds Investigated by Theoretical and Solid-State NMR**

**CHART 2: Molecular Structures of the *trans*- and *cis*-Diphosphetes**


Experimental: R = *tert*-butyl

Calculated: R = H

phosphorane,<sup>21</sup> **4**. More recently, the <sup>31</sup>P CS tensor of 3-dichloromethylene-*trans*-1,2-bis(2,4,6-tri-*tert*-butylphenyl)-1,2-diphosphirane, **5**, was reported.<sup>22</sup> The structures of the latter compounds are illustrated in Chart 1. These studies involve three-membered ring systems containing phosphorus; we are not aware of any reports of <sup>31</sup>P CS tensors in four-membered heterocyclic systems, although Albrand et al. investigated a series of cyclotetraphosphanes oriented in liquid-crystalline solvents.<sup>23,24</sup> In this study, we have examined the <sup>31</sup>P NMR spectra of solid samples of *trans*- and *cis*-1,2-dihydro-1-methyl-2-phenyl-3,4-bis(*tert*-butyl)-1,2-diphosphete (Chart 2), herein-after referred to as the *trans* and *cis* isomers, respectively. The structures of these compounds, as determined by X-ray crystallography,<sup>25</sup> indicate that the P–P and C–C bond lengths are within the range observed for related acyclic compounds. This observation led to the suggestion that the phosphorus lone-pair electrons are not delocalized in these 1,2-diphosphetes.

The two <sup>31</sup>P nuclei in each molecule are directly bonded and distant from <sup>31</sup>P nuclei in adjacent molecules, thus constituting an isolated spin pair under the condition of high-power proton decoupling. The presence of this spin pair provides an op-



**Figure 1.** Orientation of the applied magnetic field in the principal axis system of the CS tensor.

portunity to investigate the orientation of the CS tensor relative to the dipolar vector.<sup>26–32</sup> Finally, ab initio chemical shielding calculations are performed on model compounds of the *trans* and *cis* isomers, allowing the proposal of an orientation, in the molecular framework, of the principal components of the CS tensors for each phosphorus.

**Background Theory**

**Powder Line Shapes of AB Spin Systems in Stationary Samples.** In general, when considering two coupled spins that are not magnetically equivalent, four transitions occur for a given crystallite orientation.<sup>26–31</sup> The frequencies ( $\nu_i$ ) and intensities ( $I_i$ ) of these transitions are described by eqs 1–4.

$$\nu_1 = \frac{1}{2}(\nu_A + \nu_B + D + A) \quad I_1 = 1 - \frac{B}{D} \quad (1)$$

$$\nu_2 = \frac{1}{2}(\nu_A + \nu_B + D - A) \quad I_2 = 1 + \frac{B}{D} \quad (2)$$

$$\nu_3 = \frac{1}{2}(\nu_A + \nu_B - D + A) \quad I_3 = 1 + \frac{B}{D} \quad (3)$$

$$\nu_4 = \frac{1}{2}(\nu_A + \nu_B - D - A) \quad I_4 = 1 - \frac{B}{D} \quad (4)$$

In these equations,  $\nu_A$  and  $\nu_B$  are the resonance frequencies of spins A and B in the absence of spin–spin interactions. For example,  $\nu_A$  is defined by

$$\nu_A = \frac{\gamma B_0}{2\pi} [1 - (\sigma_{11}^A \sin^2 \theta \cos^2 \phi + \sigma_{22}^A \sin^2 \theta \sin^2 \phi + \sigma_{33}^A \cos^2 \theta)] \quad (5)$$

where  $\gamma$  is the magnetogyric ratio and the angles  $\theta$  and  $\phi$  orient the applied field,  $B_0$ , in the principal axis system of the CS tensor (Figure 1). The principal components of the CS tensor are described by  $\sigma_{ii}^A$  such that  $\sigma_{33}^A \geq \sigma_{22}^A \geq \sigma_{11}^A$ . The resonance frequency of  $\nu_B$  is related to  $\sigma_{ii}^B$  in an analogous manner. The terms A and B depend on the isotropic value of the indirect spin–spin coupling,  $J_{\text{iso}}$ , as well as on the effective dipolar coupling,  $R_{\text{eff}}$ :

$$A = J_{\text{iso}} - R_{\text{eff}}(3 \cos^2 \zeta - 1) \quad (6)$$

$$B = J_{\text{iso}} + R_{\text{eff}}(3 \cos^2 \zeta - 1)/2 \quad (7)$$

$$D = [(\nu_A - \nu_B)^2 + B^2]^{1/2} \quad (8)$$

The angle  $\zeta$  describes the orientation of the applied magnetic field relative to the dipolar vector,  $\mathbf{r}_{\text{AB}}$  (the <sup>31</sup>P–<sup>31</sup>P bond axis for the diphosphetes). Experimentally, one measures an effective

dipolar coupling that contains contributions from the direct dipolar coupling,  $R_{DD}$ , as well as from the anisotropy<sup>31</sup> in the  $\mathbf{J}$  tensor,  $\Delta J$ :

$$R_{\text{eff}} = R_{DD} - \frac{\Delta J}{3} \quad (9)$$

The former is inversely related to the cube of the internuclear separation,  $r_{AB}$ :

$$R_{DD} = \left(\frac{\mu_0}{4\pi}\right) \left(\frac{\hbar}{2\pi}\right) \gamma^2 (r_{AB}^{-3}) \quad (10)$$

where the angular brackets indicate that the observed dipolar coupling is subject to motional averaging.<sup>33</sup>

Crystallites in powder samples are arranged randomly, giving rise to the so-called powder NMR pattern. This pattern may be described by the span,  $\Omega$ , and the skew,  $\kappa$ .<sup>34</sup> The span indicates the range of the CS tensor principal components such that  $\Omega = \delta_{11} - \delta_{33}$ , whereas the skew describes the appearance of the powder line shape in terms of the relative values of the principal components,  $\kappa = 3(\delta_{22} - \delta_{\text{iso}})/\Omega$  with  $-1 \leq \kappa \leq 1$ . Since there are four NMR transitions arising from an isolated spin pair (eqs 1–4), the observed NMR spectrum of a powder sample is a superposition of four subspectra. The frequencies and intensities of these transitions depend on the orientations of the crystallites in the applied magnetic field, and in the case of an AB spin pair, may be complicated by second-order effects, resulting in complex powder patterns.<sup>26,35</sup>

With high-power proton decoupling, the  $^{31}\text{P}$  NMR spectra of stationary samples of the trans and cis isomers are dominated by the orientation-dependent nuclear shielding interactions at the phosphorus nuclei. To a lesser extent, the orientation dependence of the direct dipolar coupling between the directly bonded  $^{31}\text{P}$  nuclei will also affect the NMR line shapes. The dipolar splitting observed in a particular direction depends on the orientation of  $\mathbf{r}_{PP}$  relative to the applied magnetic field.<sup>36</sup> Hence, the dipolar splitting observed when the applied magnetic field is parallel to a particular principal component of the CS tensor offers information about the orientation of that component relative to  $\mathbf{r}_{PP}$ . The orientation of the principal components of the CS tensor, relative to the dipolar vector, may be discussed in terms of a set of Euler angles that describe the transformation from the PAS of the dipolar tensor to that of the CS tensor.<sup>37</sup> However, it is more convenient to discuss the CS tensor orientation in terms of the angles,  $\theta_{ii}$ , formed by the CS tensor components  $\delta_{ii}$  with  $\mathbf{r}_{PP}$ , and the Euler angle  $\alpha$ , which describes the relative orientation of the two CS tensors. Since in the absence of motion the dipolar tensor is axially symmetric, the calculated powder spectrum is invariant to simultaneous rotation of the two CS tensors about  $\mathbf{r}_{PP}$ . Also, eq 5 shows that two values, an angle  $\theta_{ii}$  and its supplement, will yield the same calculated frequency. A calculated powder spectrum based on the dipolar chemical shift method thus yields an infinite set of solutions, with a given tensor component oriented along one of two cones, as illustrated in Figure 2. In the absence of local site symmetry, no further information about the orientation of the CS tensor may be gained from this experiment. However, there is growing evidence that modern ab initio calculations can provide valuable insight into the orientation in the molecular frame of reference of CS tensors.<sup>32,38–40</sup>

**Line Shapes of AB Spin Systems under Conditions of Magic-Angle Spinning (MAS).** With high-power decoupling of the abundant spins under rapid MAS conditions, the NMR spectrum of an isolated spin will consist of an isotropic peak.

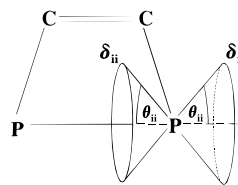


**Figure 2.** Possible orientations of a CS tensor component,  $\delta_{ii}$ , about a dipolar vector (the  $^{31}\text{P}$ – $^{31}\text{P}$  bond here), as determined by the dipolar chemical shift method. The angle formed by  $\delta_{ii}$  with the dipolar vector,  $\mathbf{r}_{PP}$ , is defined by  $\theta_{ii}$ .

However, in the case of a homonuclear spin pair, the direct dipolar interaction may not be completely averaged by MAS,<sup>41</sup> giving rise to a distribution of NMR frequencies. This has been exploited to gain information about the orientation of the CS tensor,<sup>39,42–45</sup> although the same information is usually more readily available from an analysis of the spectrum of the stationary sample (vide supra).

The Hamiltonian describing the NMR spectrum of an MAS sample is time-dependent.<sup>46</sup> By use of average Hamiltonian theory,<sup>41</sup> equations describing the spectral line shapes of MAS samples have been derived.<sup>42,47</sup> Similar to spectra of stationary samples, the observed spectrum of an MAS sample is a consequence of four NMR transitions. However, since  $^1J_{\text{iso}}(^{31}\text{P}$ – $^{31}\text{P})$  is negligible for the molecules considered here (vide infra), the observed MAS peaks may be described by two transitions:

$$\nu_{\pm} = \frac{1}{2}(\nu_{\Sigma} \pm D') \quad (11)$$

where

$$D' = [(\nu_{\Delta} - G)^2 + F^2 + K^2]^{1/2} \quad (12)$$

The terms  $\nu_{\Sigma}$  and  $\nu_{\Delta}$  are the sum and difference, respectively, of the isotropic resonance frequency of spins  $A$  and  $B$ . The parameters  $G$ ,  $F$ , and  $K$  are higher-order corrections to the average Hamiltonian:

$$G = \sum_{n=1}^{+\infty} \frac{g_{2n}}{(2\pi\nu_{\text{rot}})^{2n}}; \quad F = \sum_{n=1}^{+\infty} \frac{f_{2n}}{(2\pi\nu_{\text{rot}})^{2n}}; \quad K = \sum_{n=0}^{+\infty} \frac{k_{2n+1}}{(2\pi\nu_{\text{rot}})^{2n+1}} \quad (13)$$

where  $\nu_{\text{rot}}$  is the MAS frequency. The terms  $g_{2n}$ ,  $f_{2n}$ , and  $k_{2n+1}$  are correction coefficients that are proportional to the instantaneous chemical shift difference,  $\Delta\nu$  (in Hz):

$$g_{2n} \propto R_{DD}^{2n}(\Delta\nu); \quad f_{2n} \propto R_{DD}(\Delta\nu)^{2n}; \quad k_{2n+1} \propto R_{DD}(\Delta\nu)^{2n+1} \quad (14)$$

Exact expressions for these coefficients are given elsewhere.<sup>48</sup> They depend on the principal components of the CS tensors and  $R_{DD}$  as well as the orientation of the dipolar vector relative to the CS tensors. Equation 13 accounts for the observed dependence of the line shapes of MAS samples on  $\nu_{\text{rot}}$ . At high MAS frequencies, the terms  $G$ ,  $F$ , and  $K$  approach zero and the separation between the peaks is  $\nu_{\Delta}$ . However, eq 14 shows that the peaks of MAS samples also depend on  $\Delta\nu$ , which increases with  $B_0$ . Hence, the NMR line shapes of MAS samples may also exhibit a dependence on the applied magnetic field. Since eqs 11–14 describe the *total* line shape, it is necessary to sum the experimental spectrum over all the spinning sidebands when considering these equations.<sup>43</sup>

## Experimental Section

The preparation of the title compounds has been reported previously.<sup>25</sup> Solid-state  $^{31}\text{P}$  NMR spectra were recorded on

**TABLE 1: Summary of Basis Sets Used for *ab Initio* Calculations**

basis	P	adjacent <sup>a</sup>	phenyl ring <sup>b</sup>	other nuclei
I	3-21G	3-21G	3-21G	3-21G
II	6-31G(d)	6-31G(d)	6-31G(d)	6-31G(d)
III	6-311+G(d)	6-311+G(d)	6-31G(d)	3-21G
IV	TZ ANO <sup>56,57</sup>	3-21G	3-21G	3-21G

<sup>a</sup> Nuclei directly bonded to the phosphorus. <sup>b</sup> Carbons of the phenyl group, excluding the ipso carbon.

Bruker MSL-200 ( $B_0 = 4.7$  T) or AMX-400 ( $B_0 = 9.4$  T) NMR spectrometers operating at 81 and 162 MHz, respectively. Fine crystalline samples were packed into 7 and 4 mm o.d. zirconium oxide rotors for the 4.7 and 9.4 T spectrometers, respectively. Cross polarization (CP) under the Hartmann–Hahn match condition was used, with contact times of 2–5 ms. All spectra were acquired with high-power proton decoupling; typical  $^1\text{H}$  90° pulse widths were 4.0–5.5  $\mu\text{s}$ . Recycle times ranged from 10 to 60 s. Sample spinning frequencies ranged from 1 to 5 kHz at the lower field and from 2 to 12 kHz at the higher field. All  $^{31}\text{P}$  chemical shifts were referenced to 85%  $\text{H}_3\text{PO}_4(\text{aq})$  by setting the isotropic peak of solid  $\text{NH}_4\text{H}_2\text{PO}_4$  to +0.81 ppm. Fully proton-coupled and partially proton-decoupled solution  $^{31}\text{P}$  NMR spectra of the trans and cis isomers were acquired on a Bruker AC 250 ( $B_0 = 5.9$  T) spectrometer operating at 101 MHz.

Simulations of the spectra of stationary samples, based on eqs 1–4, were performed with a program written in this laboratory, which incorporates the POWDER routine of Alderman et al.<sup>49</sup> Both  $R_{\text{DD}}$  and  $J_{\text{iso}}$  were considered in the calculation of the line shapes, which were convoluted with a Gaussian line-broadening function. Spectra of MAS samples were simulated, with the parameters obtained from an analysis of the corresponding stationary spectra, using the program NMRLAB.<sup>50</sup> This program performs powder averaging by sampling numerous crystal orientations using the Monte Carlo method; 10 000 orientations were used in our calculations.

*Ab initio* nuclear shielding calculations were performed on an IBM RISC/6000 workstation using the gauge-independent atomic orbitals (GIAO) method<sup>51,52</sup> within the Gaussian 94 suite of programs.<sup>53</sup> To keep computational time within practical limits, calculations were performed on model compounds of the trans and cis isomers in which the *tert*-butyl groups were replaced with hydrogen atoms (Chart 2). Restricted Hartree–Fock (RHF) calculations used locally dense basis sets<sup>54,55</sup> that included the 3-21G, 6-31G(d), 6-311+G(d) basis sets and the Roos triple- $\zeta$  atomic natural orbital (TZ ANO)<sup>56,57</sup> on the phosphorus atoms. The latter is a contracted (17s,12p,5d,4f)/[6s,5p,3d,2f] basis set. These basis sets, labeled I–IV, respectively, are summarized in Table 1. The molecular structure, excluding the hydrogen atoms, is from an X-ray crystallographic investigation of the trans and cis isomers.<sup>25</sup> The relative positions of the hydrogen atoms were determined by *ab initio* geometry optimizations at the RHF/6-31G(d) level.  $^{31}\text{P}$  chemical shifts were calculated by taking the absolute shielding of 85%  $\text{H}_3\text{PO}_4(\text{aq})$  to be 328.35 ppm<sup>58</sup> (i.e.,  $\delta(\text{calc}) = 328.35 - \sigma(\text{calc})$ ).

## Results and Discussion

**$^{31}\text{P}$  CS Tensors of the Trans Isomer.** The  $^{31}\text{P}$  NMR spectra of a stationary sample of the trans isomer are shown in Figure 3 along with spectra calculated using best-fit experimental parameters. Because the  $^{31}\text{P}$  nuclei of this compound do not possess any local symmetry, assumptions cannot be made about the orientations of their CS tensors. Hence, a complete line shape

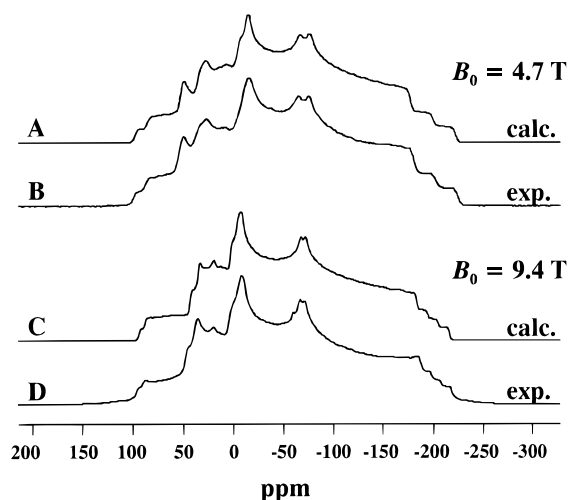


**Figure 3.** Calculated (A) and experimental (B) spectra of a stationary sample of *trans*-1,2-dihydro-1-methyl-2-phenyl-3,4-bis(*tert*-butyl)-1,2-diphosphate at  $B_0 = 4.7$  T. Traces C and D are the corresponding spectra at  $B_0 = 9.4$  T.

analysis was performed by refining the parameters describing the CS tensors, in a trial-and-error manner, and comparing the calculated and experimental spectra obtained at both 4.7 and 9.4 T. Analysis of these spectra yielded the principal components of the  $^{31}\text{P}$  CS tensors, summarized in Table 2. The spans of the CS tensors for the two nuclei are comparable, but the corresponding skewers are significantly different.

To discuss the accuracy of the calculated CS tensors, it is useful to consider calculated values for both the trans and cis isomers, summarized in Table 2. A statistical analysis of the experimental and calculated values is listed in Table 3. The correlation coefficients ( $r$ ) show that the correlation between experimental and calculated data is reasonable for all basis sets. However, the slope,  $a$ , and intercept,  $b$ , of the best-fit lines show that only basis sets III and IV correlate well with experiment (perfect agreement between experiment and theory would yield values of 1 and 0 for  $a$  and  $b$ , respectively). Plots of the magnitudes of the experimental CS tensor components versus those calculated with basis sets III and IV are shown in Figures 4 and 5. The negative intercepts for the best-fit lines of these two basis sets show that the calculated values are converging to values that are shielded by approximately 30 ppm relative to the experimental values. It is also instructive to consider the last column in Table 3, the deviations of the calculated data from the corresponding experimental values. These also show that agreement with experiment improves with the larger basis sets. Figures 3 and 4, as well as Table 3, imply that agreement with experimental results is actually better with the smaller basis set III. However, one must recall that we are comparing experimental data acquired in the solid state with calculated values for isolated molecules. Gas-phase NMR studies show that the  $^{31}\text{P}$  nucleus is usually shielded significantly compared to values obtained for the same molecule in the liquid phase.<sup>9,58</sup> In addition, *ab initio* calculations at the SCF level on  $\text{PH}_3$  show that the calculated phosphorus shielding converges to values that are shielded compared to their experimental values.<sup>59</sup> Studies suggest that the effects of electron correlations, which have not been considered in these calculations, may be important, particularly for nuclei with localized lone-pair electrons.<sup>59–64</sup> Unfortunately, it is not practical at this time to carry out such calculations on the molecules considered here. We must also consider the effect of substituting hydrogen atoms for *tert*-butyl groups on the unsaturated ring carbons. Recent



**TABLE 2: Experimental and Calculated Phosphorus Chemical Shift Tensors<sup>a,b</sup> in the 1,2-Dihydro-1,2-diphosphate Derivatives**

		$\delta_{11}$	$\delta_{22}$	$\delta_{33}$	$\delta_{\text{iso}}$	$\Omega$	$\kappa$	$\theta_{11}$	$\theta_{22}$	$\theta_{33}$	$\alpha$	
Trans Isomer												
<sup>31</sup> P-Ph	expt	38	-5	-210	-59.4	248	0.66	40	50	90	0	
	I	-132	-190	-253	-191.7	121	0.04	37	58	75	0	
	II	-62	-115	-211	-129.3	149	0.29	27	64	86	0	
	III	8	-50	-157	-66.4	165	0.30	29	62	85	0	
<sup>31</sup> P-Me	IV	-14	-63	-181	-86.0	167	0.41	26	64	86	0	
	expt	90	-70	-190	-56.4	280	-0.15	44	46	90	0	
	I	-51	-231	-253	-178.3	202	-0.78	45	79	48	81	
	II	1	-178	-213	-129.8	214	-0.68	41	50	83	21	
<sup>31</sup> P-Me	III	78	-113	-160	-65.1	238	-0.60	42	48	90	18	
	IV	52	-129	-182	-86.5	234	-0.54	40	50	90	15	
	Cis Isomer											
	<sup>31</sup> P-Ph	expt	31	-50	-108	-42.3	139	-0.17	21	70	84	0
I		-97	-179	-228	-168.0	131	-0.25	43	50	77	0	
II		-41	-133	-165	-112.7	124	-0.49	24	68	80	0	
III		30	-70	-95	-44.9	125	-0.60	28	64	83	0	
<sup>31</sup> P-Me	IV	7	-87	-118	-66.0	125	-0.50	27	63	85	0	
	expt	51	-98	-122	-56.3	173	-0.72	28	87	62	157	
	I	-33	-172	-290	-165.0	257	-0.08	50	53	62	177	
	II	2	-137	-232	-122.4	234	-0.19	40	61	65	180	
<sup>31</sup> P-Me	III	85	-75	-166	-51.9	251	-0.28	41	59	66	175	
	IV	61	-94	-184	-72.6	245	-0.26	41	57	68	172	

<sup>a</sup> All chemical shifts are in ppm. Estimated errors in the principal components are less than 5 ppm; those of the isotropic peaks are less than 0.5 ppm. <sup>b</sup> See Table 1 for a summary of the basis sets (I-IV) used for the ab initio calculations.

**TABLE 3: Statistical Comparison of the Calculated and Experimental CS Tensor Components**

basis set	$r^a$	$a^b$	$b^b/\text{ppm}$	deviation <sup>c</sup> /ppm
I	0.88	0.75	-136	136
II	0.93	0.79	-81	82
III	0.94	0.87	-11	34
IV	0.95	0.86	-32	40

<sup>a</sup> Correlation coefficients for the plot of calculated vs experimental data (Table 2). <sup>b</sup> The components of the best-fit line for the correlation between calculated and experimental data (i.e.,  $\delta_{\text{calc}} = a\delta_{\text{exp}} + b$ ). <sup>c</sup> The deviation of the calculated CS tensor components from the corresponding experimental data ( $= [(\sum(\delta_{\text{calc}} - \delta_{\text{exp}})^2)/(n - 1)]^{1/2}$  where  $n$  is the number of data points).

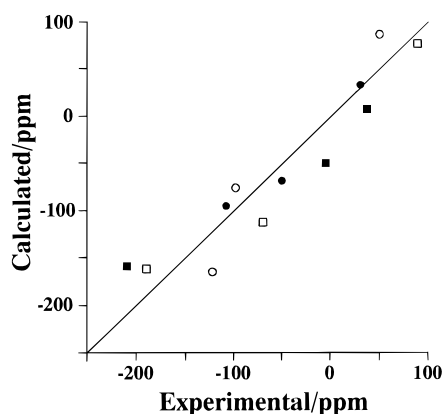


**Figure 4.** Chemical shift tensor components, calculated using basis set III, plotted vs the experimental values. The filled and open squares are the tensor components of <sup>31</sup>P-Ph and <sup>31</sup>P-Me, respectively, for the trans isomer. The filled and open circles are the corresponding values for the cis isomer. The solid line indicates points of agreement between experiment and theory—points below this line are calculated tensor components that are shielded compared to experimental values.

theoretical calculations on diphosphetes suggest that such substitutions do not have a significant effect on the molecular structure about the phosphorus atoms.<sup>65</sup> Nevertheless, the necessary simplicity of our model makes a rigorous comparison of experimental and calculated results difficult. Hence, the slightly better agreement between basis set III and experiment

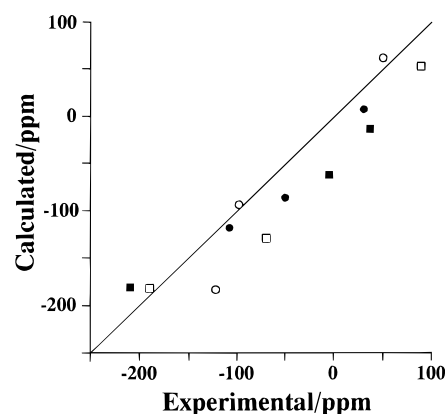


**Figure 5.** Chemical shift tensor components calculated using basis set IV plotted vs the experimental values. See the caption of Figure 4 for a description of the points.

may be fortuitous. With the above factors, we consider agreement to be good with either basis set III or IV. Finally, we note that cancellation of errors results in calculated isotropic chemical shifts that are much closer to experimental values than are the individual tensor components, particularly for basis set III, illustrating the importance of considering the individual tensor components when assessing the accuracy of a computational technique.

Analysis of the experimental spectra of the trans isomer indicates that the orientations of the two CS tensors are similar, with both  $\delta_{33}$  components perpendicular to the P-P bond (i.e.,  $\theta_{33} = 90^\circ$ ).  $\theta_{11}$  is  $40^\circ$  for <sup>31</sup>P-Ph and  $44^\circ$  for <sup>31</sup>P-Me. The corresponding values for  $\theta_{22}$  are 50 and  $46^\circ$ . The calculated orientations of the <sup>31</sup>P CS tensors of the model compound for the trans isomer are in good agreement with the experimental results (Table 2). With the exception of the lowest level calculation, the calculated orientation is virtually invariant to the basis set. Calculations on small molecules (PH<sub>3</sub><sup>59</sup> and P<sub>2</sub>H<sub>4</sub><sup>66</sup>) show that inclusion of electron correlation has a large effect on the calculated magnitudes of the CS tensor components but does not significantly alter the calculated orientations. Hence, we turn to the calculated results to propose orientations for the <sup>31</sup>P CS tensor in the molecular framework. These calculations

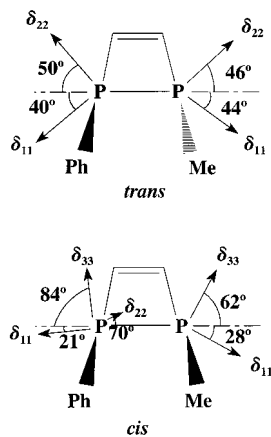


**Figure 6.** Orientation of the  $^{31}\text{P}$  CS tensors of *trans*- and *cis*-1,2-dihydro-1-methyl-2-phenyl-3,4-bis(*tert*-butyl)-1,2-diphosphate. Components perpendicular to the approximate plane of the  $\text{C}_2\text{P}_2$  rings, the  $\delta_{33}$  components of the *trans* isomer and the  $\delta_{22}$  component of  $^{31}\text{P}$ -Me of the *cis* isomer, are not shown.

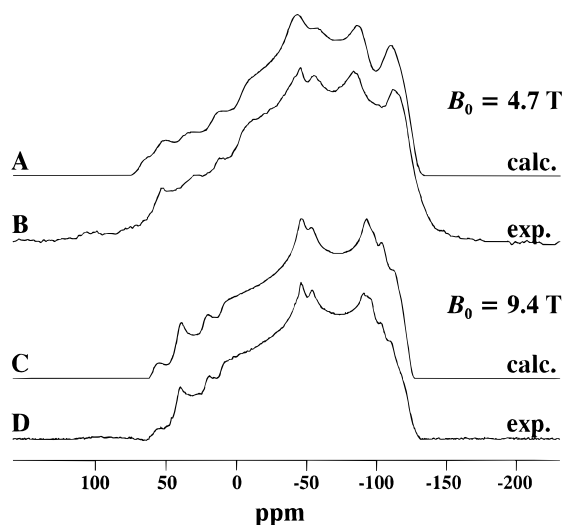


**Figure 7.** Calculated (A) and experimental (B) spectra of a stationary sample of *cis*-1,2-dihydro-1-methyl-2-phenyl-3,4-bis(*tert*-butyl)-1,2-diphosphate at  $B_0 = 4.7$  T. Traces C and D are the corresponding spectra at  $B_0 = 9.4$  T.

indicate that the  $\delta_{33}$  components are perpendicular to the approximate plane described by the  $\text{C}_2\text{P}_2$  ring.  $^{31}\text{P}$  NMR studies of three-membered heterocyclic compounds<sup>20–22</sup> have found a similar orientation for the  $\delta_{33}$  components of those  $^{31}\text{P}$  CS tensors. The remaining two principal components are oriented as shown in Figure 6.

The observed powder spectrum of an isolated spin pair is usually sensitive to  $R_{\text{eff}}$ . Given that  $\Delta J/3$  has been found to be relatively small in other systems containing P–P bonds,<sup>67</sup> it is reasonable to assume that  $R_{\text{eff}} \approx R_{\text{DD}}$  (eq 9). Hence,  $r_{\text{PP}}$  may be calculated from eq 10. The dipolar coupling constant used in the spectral simulations is 1.8 kHz, a value that is estimated to be accurate to within  $\pm 0.2$  kHz. Hence, the P–P bond length is calculated to be  $2.22 \pm 0.07$  Å, comparable to the value obtained from an X-ray diffraction study,  $2.202$  Å.<sup>25</sup>

**$^{31}\text{P}$  CS Tensors of the Cis Isomer.** The  $^{31}\text{P}$  NMR spectra of a stationary sample of the *cis* isomer are shown in Figure 7. The simulated spectra, analyzed as for the *trans* isomer, are also shown. The parameters used to calculate the spectra, with the corresponding values determined from ab initio calculations, are summarized in Table 2. The higher-level calculations predict that  $^{31}\text{P}$ -Me is more shielded than  $^{31}\text{P}$ -Ph, in agreement with

experiment (vide infra). Furthermore, the larger span of  $^{31}\text{P}$ -Me relative to  $^{31}\text{P}$ -Ph is reproduced by the ab initio calculations. The two tensors have similar relative orientations with respect to the molecular frame ( $\alpha = 157^\circ$ ). An effective dipolar coupling of 1.8 kHz was used in the calculation of the spectra, which, neglecting  $\Delta J/3$  and vibrational motion, corresponds to a P–P bond length of  $2.22 \pm 0.07$  Å, in agreement with the experimental value of  $2.218$  Å.<sup>25</sup>

Similar to results for the *trans* isomer, the calculated CS tensor orientations of the *cis* isomer are essentially invariant to basis set (Table 2). These computations suggest that the  $\delta_{33}$  components of both tensors are in the approximate plane defined by the  $\text{C}_2\text{P}_2$  ring, with the  $\delta_{22}$  components approximately perpendicular to the ring (Figure 6).

Comparison of the CS tensors in the two molecules reveals significant differences. The spans of the  $^{31}\text{P}$  CS tensors in the *trans* isomer are significantly greater than those of the corresponding tensors of the *cis* isomer (Table 2). When comparing the shielding in a particular direction, one must recall that the orientations of the  $\delta_{22}$  and  $\delta_{33}$  components in the two molecules are approximately interchanged. Hence, the shielding at  $^{31}\text{P}$ -Ph in the direction perpendicular to the  $\text{C}_2\text{P}_2$  ring is 160 ppm greater for the *trans* isomer than for the *cis* isomer (i.e.,  $\delta_{33}(\text{trans}) - \delta_{22}(\text{cis}) = -160$  ppm). Likewise, the shielding at  $^{31}\text{P}$ -Me in this direction is 92 ppm greater for the *trans* isomer. The increased shielding observed in this direction is partially offset by the decreased shielding of the  $\delta_{22}$  components of the *trans* isomer compared to the  $\delta_{33}$  components of the *cis* isomer. It is interesting to note that the least shielded components,  $\delta_{11}$ , apparently are the least sensitive to the relative orientation of the substituents, since their orientations and magnitudes in the two molecules are comparable.

Barra and Robert report a linear relationship between the span of the  $^{31}\text{P}$  CS tensor and the bond angle defining the strain at the phosphorus atom of interest.<sup>21</sup> Our results are in qualitative agreement with this observation, since the spans of the  $^{31}\text{P}$  CS tensors of both isomers investigated here are significantly smaller than those found in three-membered heterocyclic compounds<sup>20–22</sup> but comparable to that of a fused 1,2,3-benzothiadiphosphole, which contains two five-membered rings.<sup>68</sup> However, we note that ring strain cannot explain the smaller spans of the CS tensors of the *cis* isomer compared to that of the *trans* isomer, since the endocyclic bond angles at each of the phosphorus atoms are similar (*trans*,  $75.9^\circ$  and  $76.4^\circ$ ; *cis*,  $76.2^\circ$  and  $76.9^\circ$ ).<sup>25</sup>

The  $\text{C}_2\text{P}_2$  ring of the *trans* isomer is distorted slightly, with a C–P–P–C torsion angle of  $9.9^\circ$ . The corresponding value for the *cis* isomer is  $1.6^\circ$ . However, the angles formed by the substituents with the approximate plane defined by the four-membered ring are comparable.<sup>25</sup> Hence, the major structural difference between the two compounds is the relative orientation of the two substituents about the P–P bond.

**AB Features in NMR Spectra of a Stationary Sample of the Trans Isomer.** Spectra of a dipolar-coupled spin pair that have comparable chemical shifts at certain crystallite orientations may contain unusual (AB) features.<sup>29,30</sup> Such characteristics are observed in the spectra of stationary samples of the *trans* isomer (Figure 3). They are most evident in the spectrum acquired at 4.7 T, a consequence of the smaller chemical shift difference (in Hz) between the two nuclei at this magnetic field strength. Such features were predicted in early studies<sup>26,27</sup> and have since been observed experimentally.<sup>29,30</sup>

The low-frequency regions of stationary spectra of the *trans* isomer (Figure 3) arise from crystallites oriented such that  $\delta_{33}$

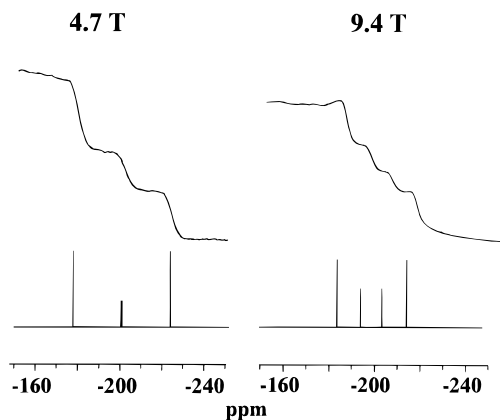


**Figure 8.**  $\delta_{33}$  region of spectra of a stationary sample of the trans isomer (upper trace) compared with the hypothetical spectra of a single crystal oriented such that  $\delta_{33}$  is along  $B_0$ .

is parallel to  $B_0$ . This region of the spectrum acquired at 4.7 T is characterized by three shoulders of about equal intensity. The corresponding region of the spectrum acquired at 9.4 T contains four shoulders, with the outer shoulders of significantly greater intensity than the inner ones. To understand the factors giving rise to the observed line shape, the spectra of a hypothetical single crystal oriented such that the  $\delta_{33}$  components are parallel to  $B_0$  (Figure 8) were calculated using eqs 1–4. These spectra accurately reproduce the shoulder positions and relative intensities observed in the NMR spectra of the powder sample and illustrate that the central shoulder of the 4.7 T spectrum is actually a superposition of the two inner peaks. Contrary to the “AB quartet” observed in NMR studies of solutions,<sup>69</sup> where the inner peaks are always more intense than the outer ones, the outer peaks are of greater intensity here. This can be understood by considering the orientation of the CS tensors. Since the orientations of the  $\delta_{33}$  components of the two  $^{31}\text{P}$  CS tensors of the trans isomer are coincident, the difference in the chemical shifts when  $B_0$  is along this direction corresponds to the difference between the two  $\delta_{33}$  components; approximately 20 ppm or 1.6 and 3.2 kHz at 4.7 and 9.4 T, respectively. Since  $\theta_{33} = 90^\circ$ , the effective dipolar coupling in this direction is 1.8 kHz (i.e.,  $\pm R_{\text{eff}}(3 \cos^2 \theta_{33} - 1) = \mp R_{\text{eff}}$ ). Clearly, the chemical shift difference between the two  $^{31}\text{P}$  nuclei is not significantly greater than  $R_{\text{eff}}$  at either field strength. Therefore, second-order effects must be considered when discussing the spectral features in this direction. These effects can be understood in terms of eqs 1–4; since  $\theta_{33} = 90^\circ$  and  $1/2 R_{\text{eff}} \gg J_{\text{iso}}$ ,  $B$  is negative (eq 7). Hence,  $I_1 = I_4 > 1$  (eqs 1 and 4) and  $I_2 = I_3 < 1$  (eqs 2 and 3). Dipolar-coupled AB spectra of this type were previously observed in  $^{13}\text{C}$  NMR spectra of a single crystal of diammonium oxalate- $^{13}\text{C}_2$ .<sup>27</sup> Here, we see that similar effects may also be observed in spectra of a powder sample.

**$^{31}\text{P}$  NMR Spectra of MAS Samples.**  $^{31}\text{P}$  NMR spectra of MAS samples of the trans and cis isomers, with the corresponding calculated spectra, are shown in Figures 9 and 10, respectively. The isotropic peaks of the trans isomer are at  $-56.4$  and  $-59.4$  ppm, while those of the cis isomer are at  $-42.3$  and  $-56.3$  ppm. Uncertainties are estimated to be less than 0.5 ppm. Selective decoupling of the phenyl ring  $^1\text{H}$  in solution  $^{31}\text{P}$  NMR spectra indicates that  $^{31}\text{P}$ –Ph of the trans isomer is more shielded than  $^{31}\text{P}$ –Me and that the assignment is reversed for the cis isomer. The latter observation is consistent with previous studies of phenyl- and methyl-substituted phosphorus nuclei, which found that  $^{31}\text{P}$ –Me is shielded by approximately 18 ppm relative to  $^{31}\text{P}$ –Ph.<sup>2,3</sup> The calculated chemical shifts of the  $^{31}\text{P}$  nuclei in these compounds (Table 2) are in qualitative agreement

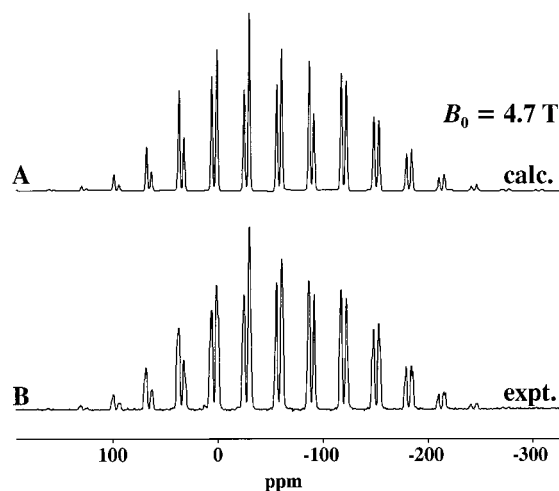


**Figure 9.** Calculated (A) and experimental (B) spectra of a MAS sample of *trans*-1,2-dihydro-1-methyl-2-phenyl-3,4-bis(*tert*-butyl)-1,2-diphosphate at  $\nu_{\text{rot}} = 2.5$  kHz and  $B_0 = 4.7$  T.

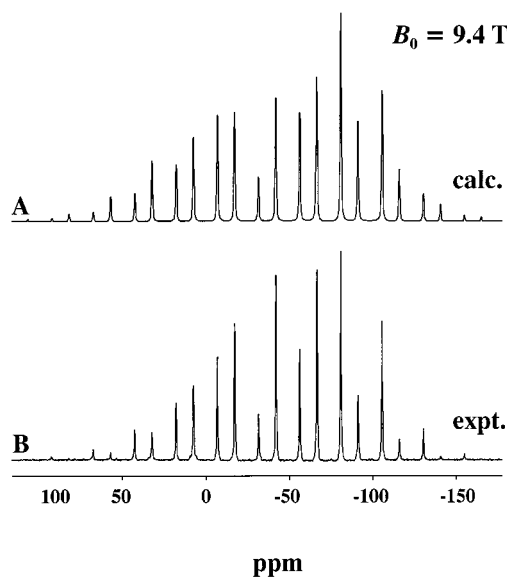


**Figure 10.** Calculated (A) and experimental (B) spectra of a MAS sample of *cis*-1,2-dihydro-1-methyl-2-phenyl-3,4-bis(*tert*-butyl)-1,2-diphosphate at  $\nu_{\text{rot}} = 4$  kHz and  $B_0 = 9.4$  T.

with the assignment of the isotropic peaks as discussed above. Splittings due to  $^1J(^{31}\text{P}$ – $^{31}\text{P})$  are not detected in either spectrum, indicating that these values must be significantly less than the line width of 100 Hz. This is consistent with the solution  $^{31}\text{P}$  NMR studies, which indicate that  $^1J(^{31}\text{P}$ – $^{31}\text{P})$  is 44 and 63 Hz for the trans and cis isomers, respectively. The presence of intense spinning sidebands observed in these spectra at moderate MAS frequencies (Figures 9 and 10) confirms that the spans of the  $^{31}\text{P}$  CS tensors are relatively large.

The individual peaks in the  $^{31}\text{P}$  MAS NMR spectra of the trans isomer are broader than those of the cis isomer and exhibit asymmetric line shapes at low MAS frequencies (Figure 9). This is more apparent in Figure 11, which shows the MAS line shapes of the trans and cis isomers with all spinning sidebands summed into the isotropic peaks. The asymmetric peaks of the trans isomer arise from the fact that at certain crystallite orientations, the chemical shift difference between the two phosphorus nuclei is comparable to the dipolar coupling between them. The case discussed above, in which the crystallites are oriented such that the four-membered ring is perpendicular to  $B_0$ , is an example of this. The symmetric line shapes of the MAS peaks of the cis

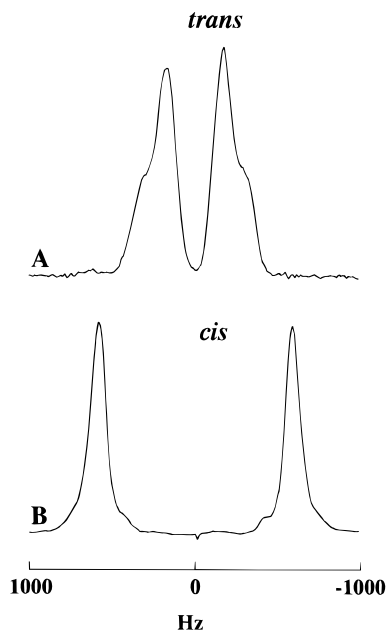


**Figure 11.** Total line shapes of the  $^{31}\text{P}$  NMR spectra of MAS samples of the trans and cis isomers at  $B_0 = 4.7$  T and  $\nu_{\text{rot}} = 4$  kHz. For comparison, the spectra are arbitrarily centered at 0 Hz.

isomer suggest that there are few, if any, orientations in which the chemical shifts of the two nuclei are similar. For example, crystallites of the cis isomer oriented such that the four-membered ring is perpendicular to  $B_0$  have the  $\delta_{22}$  components approximately parallel to  $B_0$ . The chemical shift difference between the two nuclei in this orientation is approximately 4 and 8 kHz at 4.7 and 9.4 T, respectively, significantly greater than the dipolar coupling of 1.8 kHz. Hence, the effect on the MAS spectra is much less significant in this case.

The calculated MAS spectra (Figures 9A and 10A) qualitatively reproduce the experimental spectra. The spinning sideband pattern, which approximates the powder spectrum at low MAS frequencies, is accurately reproduced. The line shapes of the isotropic peaks are in qualitative agreement. In particular, the asymmetric peaks observed for spectra of the trans isomer appear to be simulated correctly.

The line widths at half-height in the spectra shown in Figure 11 are 190 and 110 Hz for the trans and cis isomers, respectively. The line widths of the total MAS peaks in the spectra of the trans isomer show a strong dependence on  $\nu_{\text{rot}}$ . For example, for spectra obtained at 4.7 T, the line widths of the isotropic peaks of both phosphorus nuclei reach a maximum of approximately 210 Hz at  $\nu_{\text{rot}} = 3.0$  kHz and decrease at faster or slower MAS frequencies. A similar pattern is observed for spectra acquired at 9.4 T. A dependence on  $\nu_{\text{rot}}$  has also been observed in other homonuclear spin pairs consisting of two nonequivalent, dipolar-coupled spins.<sup>70–73</sup> This dependence on  $\nu_{\text{rot}}$  may be understood from eq 13, which shows that the higher-order correction coefficients are inversely dependent on  $\nu_{\text{rot}}$ . Contrary to what one may expect, the maximum line width does not occur at the slowest MAS frequency, reflecting the different dependence on  $\Delta\nu$  of the correction terms. In contrast to the line widths of MAS spectra of the trans isomer, those of the cis isomer are nearly independent of  $\nu_{\text{rot}}$ , probably because of the larger  $\nu_{\Delta}$ , which partially quenches the effect of the MAS frequency-dependent terms in eq 12. Although the NMR line widths of MAS samples often increase with  $B_0$ ,<sup>74</sup> the opposite effect is observed here. This may be understood by considering eqs 11 and 12; since  $\nu_{\Delta}$  increases with the field strength, the line broadening due to the  $G$ ,  $F$ , and  $K$  terms is partially

quenched. This phenomenon has been observed previously in the MAS spectra of dipolar-coupled spin pairs.<sup>70</sup>

## Conclusions

The dipolar chemical shift method has been used to determine the magnitudes of the principal components of the  $^{31}\text{P}$  CS tensors of trans- and cis-substituted diphosphetes, as well as their orientations relative to the dipolar vector. The relative orientations of the phenyl and methyl substituents have a large effect on the orientations and magnitudes of the CS tensors. When the substituents are trans to one another, the spans of the CS tensors are over 100 ppm larger than when they are cis to one another. Spectral features, observed in the NMR spectra of MAS and stationary samples, have been interpreted in terms of the detailed theory governing homonuclear dipolar-coupled spin pairs.

There are significant discrepancies between the magnitudes of the calculated and experimental CS tensor components, perhaps because the effects of electron correlation have not been considered in the ab initio calculations. Clearly, higher-order calculations are required. Nevertheless, the calculated orientations of the principal components of the CS tensors relative to the dipolar vector are in reasonable agreement with experimental findings and are essentially invariant to basis set size. Hence, an orientation in the molecular framework, based on the combined experimental–theoretical results, has been proposed. In general, we have observed that  $^{31}\text{P}$  CS tensors in diphosphetes are very sensitive to isomerism. It is hoped that this work will initiate further studies, both experimental and theoretical, of phosphorus nuclei in strained environments.

**Acknowledgment.** We are grateful to members of the solid-state NMR group and to Dr. Klaus Eichele for helpful suggestions. R.E.W. thanks the Natural Sciences and Engineering Research Council (NSERC) of Canada for operating and equipment grants and the Canada Council for a Killam Research Fellowship. G.M.B. thanks NSERC, the Izaak Walton Killam Trust, and the Walter C. Sumner Foundation for postgraduate scholarships. All NMR spectra were obtained at the Atlantic Region Magnetic Resonance Centre (ARMRC), which is also supported by NSERC.

## References and Notes

- (1) Tebby, J. C. In *Phosphorus-31 NMR Spectroscopy in Stereochemical Analysis*; Verkade, J. G., Quin, L. D., Eds.; VCH Publishers Inc.: Deerfield Beach, FL, 1987; Chapter 1.
- (2) Quin, L. D.; Hughes, A. N. In *The Chemistry of Organophosphorus Compounds*; Hartley, F. R., Ed.; John Wiley & Sons: Chichester, 1990; Vol. 1, p 301.
- (3) Berger, S.; Braun, S.; Kalinowski, H. *NMR Spectroscopy of the Non-Metallic Elements*; John Wiley & Sons: Chichester, 1997; Chapter 7.
- (4) Kutzelnigg, W.; Fleischer, U.; Schindler, M. *NMR: Basic Princ. Prog.* **1990**, 23, 165.
- (5) Dixon, K. R. In *Multinuclear NMR*; Mason, J., Ed.; Plenum Press: New York, 1987; p 369.
- (6) Haeberlen, U. In *Advances in Magnetic Resonance, Supplement 1*; Waugh, J. S., Ed.; Academic Press: New York, 1976.
- (7) Mehring, M. *NMR: Basic Princ. Prog.* **1976**, 11, 1.
- (8) Schmidt-Rohr, K.; Spiess, H. W. *Multidimensional Solid-State NMR and Polymers*; Academic Press: London, 1994.
- (9) Heckmann, G.; Fluck, E. *Mol. Phys.* **1972**, 23, 175.
- (10) Quin, L. D.; Caster, K. C.; Kivalus, J. C.; Mesch, K. A. *J. Am. Chem. Soc.* **1984**, 106, 7021.
- (11) Chesnut, D. B.; Quin, L. D.; Moore, K. D. *J. Am. Chem. Soc.* **1993**, 115, 11984.
- (12) Nyulászai, L. *J. Phys. Chem.* **1996**, 100, 6194.
- (13) Chesnut, D. B.; Quin, L. D. *J. Am. Chem. Soc.* **1994**, 116, 9638.
- (14) Charrier, C.; Bonnard, H.; de Lauzon, G.; Mathey, F. *J. Am. Chem. Soc.* **1983**, 105, 6871.
- (15) Ramsey, N. F. *Phys. Rev.* **1950**, 77, 567.



- (16) Ramsey, N. F. *Phys. Rev.* **1950**, *78*, 699.
- (17) Grutzner, J. B. In *Recent Advances in Organic NMR Spectroscopy*; Lambert, J. B., Rittner, R., Eds.; Norell Press: Landisville, NJ, 1987; Chapter 2.
- (18) Jameson, C. J.; Mason, J. In *Multinuclear NMR*; Mason, J., Ed.; Plenum Press: New York, 1987; Chapter 3.
- (19) Duncan, T. M. *Principal Components of Chemical Shift Tensors: A Compilation*; Farragut Press: Chicago, 1994.
- (20) Barra, A. L.; Robert, J. B. *Chem. Phys. Lett.* **1987**, *136*, 224.
- (21) Barra, A. L.; Robert, J. B. *Chem. Phys. Lett.* **1988**, *149*, 363.
- (22) Challoner, R.; McDowell, C. A.; Yoshifuji, M.; Toyota, K.; Tossell, J. A. *J. Magn. Reson.* **1993**, *104A*, 258.
- (23) Albrand, J. P.; Cogne, A.; Robert, J. B. *J. Am. Chem. Soc.* **1978**, *100*, 2600.
- (24) Albrand, J. P.; Cogne, A.; Gagnaire, D.; Robert, J. B. *Mol. Phys.* **1976**, *31*, 1021.
- (25) Maignot, N.; Ricard, L.; Charrier, C.; Le Goff, P.; Mathey, F. *Bull. Soc. Chim. Fr.* **1992**, *129*, 76.
- (26) Zilm, K. W.; Grant, D. M. *J. Am. Chem. Soc.* **1981**, *103*, 2913.
- (27) van Willigen, H.; Griffin, R. G.; Haberkorn, R. A. *J. Chem. Phys.* **1977**, *67*, 5855.
- (28) Power, W. P.; Wasylishen, R. E. *Ann. Rep. NMR Spectrosc.* **1991**, *23*, 1.
- (29) Curtis, R. D.; Hilborn, J. W.; Wu, G.; Lumsden, M. D.; Wasylishen, R. E.; Pincock, J. A. *J. Phys. Chem.* **1993**, *97*, 1856.
- (30) Lumsden, M. D.; Wu, G.; Wasylishen, R. E.; Curtis, R. D. *J. Am. Chem. Soc.* **1993**, *115*, 2825.
- (31) Wasylishen, R. E. In *Encyclopedia of Nuclear Magnetic Resonance*; Grant, D. M., Harris, R. K., Eds.; John Wiley & Sons: Chichester, 1996; p 1685.
- (32) Wasylishen, R. E.; Curtis, R. D.; Eichele, K.; Lumsden, M. D.; Penner, G. H.; Power, W. P.; Wu, G. In *Nuclear Magnetic Shieldings and Molecular Structure*; Tossell, J. A., Ed.; Kluwer Academic Publishers: Dordrecht, 1993; p 297.
- (33) Ishii, Y.; Terao, T.; Hayashi, S. *J. Chem. Phys.* **1997**, *107*, 2760.
- (34) Mason, J. *Solid State Nucl. Magn. Reson.* **1993**, *2*, 285.
- (35) Lumsden, M. D.; Wasylishen, R. E.; Britten, J. F. *J. Phys. Chem.* **1995**, *99*, 16602.
- (36) Eichele, K.; Wasylishen, R. E. *J. Magn. Reson.* **1994**, *106A*, 46.
- (37) For a discussion of Euler angles, see ref 8, p 444.
- (38) Facelli, J. C. In *Encyclopedia of Nuclear Magnetic Resonance*; Grant, D. M., Harris, R. K., Eds.; John Wiley & Sons: Chichester, 1996; p 4327.
- (39) Bernard, G. M.; Wu, G.; Wasylishen, R. E. *J. Phys. Chem. A* **1998**, *102*, 3184.
- (40) Jameson, C. J. In *Nuclear Magnetic Resonance—A Specialist Periodical Report*; Webb, G. A., Ed.; The Royal Society of Chemistry: Cambridge, U.K., 1998; Vol. 27 and previous volumes of this annual series.
- (41) Maricq, M. M.; Waugh, J. S. *J. Chem. Phys.* **1979**, *70*, 3300.
- (42) Wu, G.; Wasylishen, R. E. *J. Magn. Reson.* **1993**, *102A*, 183.
- (43) Wu, G.; Wasylishen, R. E. *J. Chem. Phys.* **1993**, *99*, 6321.
- (44) Wu, G.; Sun, B.; Wasylishen, R. E.; Griffin, R. G. *J. Magn. Reson.* **1997**, *124*, 366.
- (45) Dusold, S.; Klaus, E.; Sebald, A.; Bak, M.; Nielsen, N. C. *J. Am. Chem. Soc.* **1997**, *119*, 7121.
- (46) Griffin, R. G. In *Encyclopedia of Nuclear Magnetic Resonance*; Grant, D. M., Harris, R. K., Eds.; John Wiley & Sons: Chichester, 1996; p 4174.
- (47) Wu, G.; Eichele, K.; Wasylishen, R. E. In *Phosphorus-31 NMR Spectral Properties in Compound Characterization and Structural Analysis*; Quin, L. D., Verkade, J. G., Eds.; VCH Publishers Inc.: New York, 1994; p 441.
- (48) Wu, G.; Wasylishen, R. E. *J. Chem. Phys.* **1993**, *98*, 6138.
- (49) Alderman, D. W.; Solum, M. S.; Grant, D. M. *J. Chem. Phys.* **1986**, *84*, 3717.
- (50) Sun, B.; Griffin, R. G. Unpublished results.
- (51) Ditchfield, R. *Mol. Phys.* **1974**, *27*, 789.
- (52) Wolinski, K.; Hinton, J. F.; Pulay, P. *J. Am. Chem. Soc.* **1990**, *112*, 8251.
- (53) Frisch, M. J.; Trucks, G. W.; Schlegel, H. B.; Gill, P. M. W.; Johnson, B. G.; Robb, M. A.; Cheeseman, J. R.; Keith, T.; Petersson, G. A.; Montgomery, J. A.; Raghavachari, K.; Al-Laham, M. A.; Zakrzewski, V. G.; Ortiz, J. V.; Foresman, J. B.; Cioslowski, J.; Stefanov, B. B.; Nanayakkara, A.; Challacombe, M.; Peng, C. Y.; Ayala, P. Y.; Chen, W.; Wong, M. W.; Andres, J. L.; Replogle, E. S.; Gomperts, R.; Martin, R. L.; Fox, D. J.; Binkley, J. S.; Defrees, D. J.; Baker, J.; Stewart, J. P.; Head-Gordon, M.; Gonzalez, C.; Pople, J. A. *Gaussian 94*, revision, B.2; Gaussian, Inc.: Pittsburgh, PA, 1995.
- (54) Chesnut, D. B.; Rusiloski, B. E.; Moore, K. D.; Egolf, D. A. *J. Comput. Chem.* **1993**, *14*, 1364.
- (55) Chesnut, D. B.; Moore, K. D. *J. Comput. Chem.* **1989**, *10*, 648.
- (56) Basis sets were obtained from the Extensible Computational Chemistry Environment Basis Set Database, version 1.0, as developed and distributed by Molecular Science Computing Facility, Environmental and Molecular Sciences Laboratory, which is part of the Pacific Northwest Laboratory, P.O. Box 999, Richland, WA 99352, and funded by the U.S. Department of Energy. The Pacific Northwest Laboratory is a multiprogram laboratory operated by the Battelle Institute for the U.S. Department of Energy under Contract DE-AC06-76RLO 1830. Contact David Feller, Karen Schuchardt, or Don Jones for further information.
- (57) Widmark, P.; Persson, B. J.; Roos, B. O. *Theor. Chim. Acta* **1991**, *79*, 419.
- (58) Jameson, C. J.; De Dios, A.; Jameson, A. K. *Chem. Phys. Lett.* **1990**, *167*, 575.
- (59) Wolinski, K.; Hsu, C.-L.; Hinton, J. F.; Pulay, P. *J. Chem. Phys.* **1993**, *99*, 7819.
- (60) Schindler, M. *J. Am. Chem. Soc.* **1987**, *109*, 5950.
- (61) Bouman, T. D.; Hansen, A. E. *Chem. Phys. Lett.* **1990**, *175*, 292.
- (62) Cybulski, S. M.; Bishop, D. M. *J. Chem. Phys.* **1993**, *98*, 8057.
- (63) Chesnut, D. B.; Rusiloski, B. E. In *Phosphorus-31 NMR Spectral Properties in Compound Characterization and Structural Analysis*; Quin, L. D., Verkade, J. G., Eds.; VCH Publishers: New York, 1994; p 3.
- (64) Chesnut, D. B.; Byrd, E. F. C. *Heteroat. Chem.* **1996**, *7*, 307.
- (65) Schoeller, W. W.; Tubbesing, U.; Rozhenko, A. B. *Eur. J. Inorg. Chem.* **1998**, 951.
- (66) Unpublished results from this laboratory.
- (67) Eichele, K.; Wu, G.; Wasylishen, R. E.; Britten, J. F. *J. Phys. Chem.* **1995**, *99*, 1030.
- (68) Wu, G.; Wasylishen, R. E.; Power, W. P.; Baccolini, G. *Can. J. Chem.* **1992**, *70*, 1229.
- (69) See, for example, the following. Harris, R. K. *Nuclear Magnetic Resonance Spectroscopy*; John Wiley & Sons: New York, 1986; p 47.
- (70) Wu, G.; Wasylishen, R. E. *Inorg. Chem.* **1994**, *33*, 2774.
- (71) Lindner, E.; Fawzi, R.; Mayer, H. A.; Eichele, K.; Hiller, W. *Organometallics* **1992**, *11*, 1033.
- (72) Hayashi, S.; Hayamizu, K. *Chem. Phys.* **1991**, *157*, 381.
- (73) Power, W. P.; Wasylishen, R. E. *Inorg. Chem.* **1992**, *31*, 2176.
- (74) VanderHart, D. L.; Earl, W. L.; Garroway, A. N. *J. Magn. Reson.* **1981**, *44*, 361.